RASĀYAN *J. Chem.*
Vol. 19 | No. 4 | 2276-2287 | October-December | 2026
ISSN: 0974-1496 | e-ISSN: 0976-0083 | CODEN: RJCABP
http://www.rasayanjournal.com
http://www.rasayanjournal.co.in

RICE HUSK BIOCHAR–HYDROGEL COMPOSITE AS A SLOW/CONTROLLED-RELEASE FERTILIZER: DESIGN FOR EFFICIENT POTASSIUM DELIVERY AND ENHANCED BIODEGRADABILITY

H.Hendrawan✉, A.R. Idauli, H.A. Aziz, and F. Khoerunnisa
Department of Chemistry, Universitas Pendidikan Indonesia, Bandung 4015, Indonesia
✉Corresponding author: hendrawan@upi.edu

ABSTRACT

Sustainable crop production requires fertilizers that synchronize nutrient release with plant demand while minimizing leaching. Here, we introduce a biochar–hydrogel smart slow/controlled-release fertilizers (S/CRFs) engineered from rice husk biochar and Poly(vinyl alcohol)/borate/alginate (PVA/B/A) hydrogel. The prepared S/CRFs were characterized in terms of their functional groups, pore structure, elemental composition, swelling behaviour, water-retention capacity, nutrient-release performance, and biodegradability. Performance evaluation revealed that increasing the impregnation time reduced biochar porosity and was accompanied by lower swelling and water-retention capacities. Granules prepared with biochar impregnated for 48 h exhibited the slowest potassium release, reaching 89.47% cumulative release after 42 days in soil. The release behaviour was best described by the pseudo-second-order kinetic model. Biodegradability tests confirmed progressive disintegration within 70 days, supporting their environmental compatibility. The combined use of KCl-impregnated biochar, a hydrogel matrix, and a hydrogel coating created a triple-barrier release system: the biochar served as a porous nutrient-storage matrix, whereas the hydrogel functioned both as an internal nutrient reservoir and as an external diffusion-controlling coating. This strategy integrates pore confinement, diffusion control, and biodegradability, offering a scalable strategy for developing smart fertilizers with the potential to improve nutrient-use efficiency while reducing nutrient losses; thereby supporting the SDG-12.

Keywords: Biodegradability, Hydrogel Composite, Rice Husk, Slow/Controlled-Release Fertilizers, Potassium Delivery.

RASĀYAN *J. Chem.*, Vol. 19, No.4, 2026

INTRODUCTION

The intensive application of conventional soluble fertilizers has long supported global agricultural productivity, but their inefficiency is well recognised. Large fractions of applied nitrogen and phosphorus are lost to leaching, volatilisation, and runoff, contributing to eutrophication, greenhouse gas emissions, and diminished nutrient use efficiency (NUE).[1] These issues are directly linked to the achievement of the United Nations Sustainable Development Goals (SDGs), particularly SDG-12 (Responsible Consumption and Production), emphasising the need for more efficient and environmentally sustainable nutrient management strategies. The development of slow/controlled-release fertilizers (S/CRFs) has therefore become a critical research area to synchronise nutrient availability with plant uptake dynamics, reduce nutrient losses, and enhance agronomic performance. These systems often employ coatings, carriers, or hydrogel matrices to regulate nutrient release, while balancing cost, biodegradability, and scalability.[1,2] Biochar has emerged as a multifunctional component in S/CRFs owing to its high porosity, surface area, and functional groups that facilitate nutrient adsorption and gradual desorption. Rice husk-derived biochar (RHB) is particularly attractive, given rice husk's abundance, high silica content, and tuneable surface chemistry**.** RHB-based fertilizers have been shown to reduce nitrogen leaching, improve phosphorus retention, and provide sustained nutrient release.[3,4] RHB impregnated with nitrogen sources significantly slowed nitrogen release while simultaneously immobilizing cadmium, highlighting its dual agronomic and environmental benefits.[3] Field and pot trials confirm that RHB-coated urea improves soil fertility and NUE more than uncoated fertilizers.[5] Hydrogels are another promising approach for nutrient delivery, functioning as three-dimensional polymer networks capable of swelling in soil moisture and releasing

This work is licensed under a CC BY 4.0 license.

entrapped fertilizers by diffusion or degradation. Natural polymers such as alginate and starch, as well as synthetic polymers such as poly(vinyl alcohol) (PVA), have been extensively studied for their ability to encapsulate urea and NPK fertilizers.[6,7] PVA provides mechanical robustness, film-forming capability, and reversible physical crosslinks, making it widely used in hydrogel-based S/CRFs.[8] Sodium alginate, in particular, forms stable gels with divalent cations (e.g., Ca^{2+}), enabling bead or matrix formation for encapsulation.[9] Alginate plays an important role in hydrogel formation by acting as a crosslinking agent. Some studies have demonstrated the capacity of PVA/alginate hydrogels to retard urea release significantly compared to unencapsulated fertilizers.[10,11] For instance, PVA–alginate–humic acid hydrogels exhibited extended urea release and improved biodegradation characteristics, showing potential as soil conditioners.[12]

Borate ions form dynamic diol-borate complexes with PVA hydroxyl groups, yielding reversible, physically crosslinked networks with tuneable swelling, mechanical strength, and self-healing capacity.[13] Under repeated dry–rewet cycles, sodium tetrahydroxyborate crosslinked poly(vinyl alcohol) and alginate form a shape-stable hydrogel at pH higher than nine.[14] Compared to glutaraldehyde crosslinking, borate crosslinking is less toxic and more environmentally benign, aligning better with sustainable agricultural applications.[10] In addition, starch-based hydrogels crosslinked with borate effectively reduced the release rate of urea from hours to several days.[7] These findings highlight the potential of combining PVA, alginate, and borate crosslinkers to fine-tune hydrogel performance for S/CRFs. Integrating rice husk biochar and PVA/borate/alginate hydrogels offers complementary benefits for S/CRFs design. Biochar's microporosity provides storage sites for nutrient ions and mitigates burst release, while the hydrogel matrix further regulates diffusion through swelling and moisture-responsive behaviour. This synergy enhances nutrient use efficiency and reduces environmental losses, while simultaneously improving soil water retention and contributing trace elements such as silica. Moreover, both biochar and hydrogel components are derived from relatively low-cost feedstocks and can be scaled with existing agricultural and polymer technologies.

Although the potential of this hybrid system has been recognized, systematic investigations into the interactions among biochar feedstock, pyrolysis temperature, surface modification, fertilizer loading methods, and hydrogel formulation parameters (PVA/alginate ratio, borate concentration, and crosslink density) remain scarce.[15] In particular, studies focusing on nutrient-release kinetics are still limited. This study therefore develops a composite S/CRFs in which rice husk-derived biochar serves as a nutrient carrier embedded within and/or coated by a PVA/borate/alginate hydrogel matrix. Physicochemical characterisation, nutrient release modelling, and fertilizers performance evaluation are conducted to establish design–function relationships and assess the potential of this hybrid system to enhance controlled nutrient release, mitigate nutrient losses, and promote sustainable crop production.

EXPERIMENTAL

Materials and Methods

Poly(vinyl alcohol) (PVA, Mw 60,000 g/mol), sodium borate ($Na_2B_4O_7$), sodium alginate, and potassium chloride (KCl, Merck) were used as raw materials. Biochar was prepared by pyrolysing local rice husk in a furnace (Uchida IMF 72, Japan). Deionised water was used throughout the study.

General Procedure

Preparation of Rice Husk-Derived Biochar

Rice husks were pyrolysed at 400 °C for 30 minutes to obtain biochar, which was ground (70 mesh), washed, and dried at 50 °C. A portion of biochar was impregnated with saturated KCl solution under stirring at room temperature for 24 h and 48 h. The impregnated samples were filtered, rinsed, and dried at 50 °C. The resulting materials were designated BCI_{24} (biochar impregnated for 24 h) and BCI_{48} (biochar impregnated for 48 h).

Preparation of S/CRFs Granule

Granules of S/CRFs were prepared by mixing untreated biochar (BC) or impregnated biochar (BCI_{24}, BCI_{48}) with KCl powder, followed by the addition of the binder, namely poly(vinyl alcohol)/borate/alginate (PVA/B/A) hydrogel solution. The mixture was granulated, dried at room

temperature, and oven-dried at 50 °C, to produce BC-A-G, BCI_{24}-A-G, and BCI_{48}-A-G. For coated variants, the granules were immersed in (PVA/B/A) hydrogel solution and dried at 50 °C to produce BC-A-G-E, BCI_{24}-A-G-E, and BCI_{48}-A-G-E.

Sorption Capacity of RHB

The sorption capacity of RHB was determined from the mass difference of the sample before and after KCl impregnation. Subsequently, KCl desorption from the RHB into deionized water was monitored by periodically measuring the electrical conductivity of the solution.

Swelling Ratio and Water Retention of S/CRFs Granule

The swelling ratio (*SR*) of coated granules was obtained by immersing dried samples (W_0) in deionized water for 3 h and reweighing (W_t), calculated using equation (1):

$$(\%SR) = \frac{W_t - W_0}{W_0} \times 100\% \quad (1)$$

Water retention (*WR*) was determined by periodic weighing during drying until a constant mass (W_∞) was reached, calculated using equation (2):

$$\%WR = \frac{(W_t - W_\infty)}{(W_0 - W_\infty)} \times 100\% \quad (2)$$

Release Behaviour of KCl from S/CRFs Granule

In aqueous medium, granules were immersed in 500 mL deionized water under stirring (200 rpm). Conductivity was recorded at 30 s intervals to monitor KCl release. In soil medium, granules were buried in soil maintained at near-saturation by daily irrigation with 10 mL deionized water. Samples were recovered at selected intervals (0, 0.5, 1, 7, 14, 28, 42 days), digested in aqua regia, and analysed for residual K^+ by AAS.

Biodegradability of S/CRFs Granule

Biodegradability was assessed by incubating granules in soil under natural conditions. Structural degradation was monitored periodically through visual inspection.

Characterization Techniques

Functional groups and vibrational modes of RHB were characterized using Fourier Transform Infrared Spectroscopy (FT-IR) (Bruker Alpha II, Germany). The surface area and pore volume of the RHB were determined using a Brunauer–Emmett–Teller (BET) surface area analyzer (Quantachrome Nova, USA). The elemental composition of the RHB was determined using X-ray Fluorescence (XRF) Spectrometry (S8 Tiger Bruker, USA). The conductivity of the solution was measured using a conductivity meter (Mettler Toledo LE703, UK). The potassium content of the soil was determined using atomic absorption spectroscopy (AAS) (Qualitest type WFX-130A, China).

RESULTS AND DISCUSSION

Physicochemical Characteristics of Rice Husk-Derived Biochar and S/CRFs Granules

Vibrational/Functional Group

The FTIR spectra of raw rice husk and its derived biochar (Fig.-1) demonstrate significant structural transformations after pyrolysis at 400 °C. The broad absorption band at 3,314 cm^{-1} in raw rice husk, attributed to O–H stretching of hydroxyl groups in cellulose, hemicellulose, and lignin, nearly disappeared in biochar. This decline indicates dehydration and thermal decomposition of hydroxyl-rich functionalities during carbonisation, consistent with dehydration and decarboxylation pathways reported in lignocellulosic pyrolysis.[16,17] The C–H stretching band at 2920 cm^{-1}, representing aliphatic structures, also diminished in biochar, confirming cleavage of alkyl chains and volatilization of low-molecular-weight organics.[18,19] Such structural losses are linked to the release of volatile organic compounds during pyrolysis, which progressively converts biomass into a condensed aromatic network. The carbonyl absorption at 1730 cm^{-1} in raw rice husk, typically arising from ester and hemicellulose-derived carbonyls, shifted to 1707 cm^{-1} with reduced intensity in biochar. This indicates partial degradation of ester/aldehyde groups, with remnants of more stable aromatic carbonyl species persisting.[20,21]

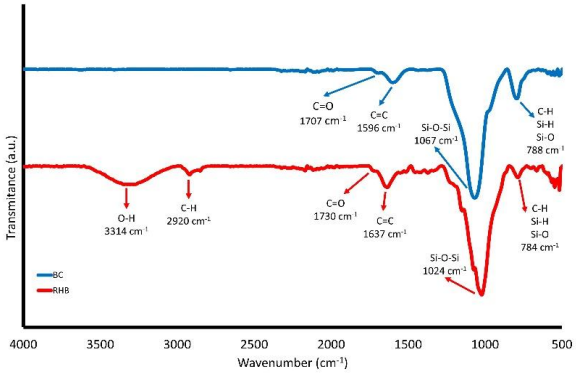


Fig.-1: FT-IR Spectra of Rice Husk and Rice Husk-Derived Biochar (RHB)

In parallel, the C=C stretching band shifted from 1637 cm^{-1} to 1596 cm^{-1} and became more intense, suggesting progressive aromatization and the development of conjugated aromatic structures.[22] In the fingerprint region, the vibrational band at 1024 cm^{-1} (Si–O–Si/C–O) shifted to 1067 cm^{-1} with increased intensity in biochar, highlighting the enrichment of silica—a dominant constituent of rice husk ash.[23,24,25] The enhanced band at ~788 cm^{-1} is associated with aromatic C–H out-of-plane deformation and/or Si–O vibrations, further supporting silica enrichment and the development of planar aromatic carbon structures.[26,27] The weak absorption features below 600 cm^{-1} are attributed to inorganic minerals and residual salts, consistent with earlier reports on rice husk biochar.[28,29] The FTIR analysis reveals the progressive transformation of rice husk biomass into a more aromatized and silica-rich carbon material through pyrolysis. The observed elimination of hydroxyl, aliphatic, and labile carbonyl groups, together with the enrichment of conjugated aromatic and silicate structures, demonstrates the enhanced recalcitrance and physicochemical stability of biochar. Such properties make rice husk biochar a promising matrix for use in slow/controlled-release fertilizers (S/CRFs) formulations, where structural integrity and nutrient-binding capacity are essential.[19]

Surface Area and Pore Volume of Rice Husk-Derived Biochar

BET analysis of rice husk biochar prepared at 400 °C (30 min, heating rate 20 °C/min) revealed a specific surface area of 126.21 m^2/g, an average pore diameter of 0.966 nm, and a pore volume of 0.197 cm^3/g. The relatively large surface area suggests that this biochar can act as an effective internal reservoir for fertilizers solutions, enhancing sorption and retention of nutrients.[30,31,32] The pore volume of 0.197 cm^3/g further supports this function, reflecting sufficient internal storage capacity for KCl solution. Nutrient release from such porous networks is expected to occur through pore diffusion and capillary-driven transport, resulting in gradual desorption rather than rapid leaching. The combination of high surface area and pore volume therefore strengthens the role of biochar as an internal component of slow/controlled-release fertilizers (S/CRFs). Increased contact area enhances impregnation efficiency and physical interactions (e.g., van der Waals forces, hydrogen bonding), while the porous reservoir helps delay nutrient release relative to low-porosity carriers.[33]

Elemental Composition of Rice Husk-Derived Biochar

XRF analysis of rice husk-derived biochar (prior to washing) revealed the presence of both macro- and micronutrients relevant to agronomic applications (Table-1). Potassium was detected at a relatively high concentration (6,368 ppm), indicating that rice husk biochar itself can act as a natural K source for plants.[34]

Table-1: Elemental Composition of Rice Husk-Derived Biochar (RHB)

Element	Concentration (ppm)	Element	Concentration (ppm)
Mo	12.34	Fe	406.23
Zr	9.34	Mn	299.52
Sr	8.73	Cr	34.23
Rb	45.65	Ca	1203.00
Zn	55.30	K	6,368.19

Micronutrients such as Fe (406 ppm), Mn (300 ppm), Zn (55 ppm), and Mo (12 ppm) were also detected, each of which plays crucial roles in plant physiology. Fe and Mn are essential for photosynthesis and electron transport, Zn contributes to enzyme activity and auxin metabolism, while Mo is a cofactor in nitrogen assimilation processes.[35,36] The XRF profile confirms that rice husk biochar is enriched with beneficial macro- and micronutrients while free of toxic elements at concerning levels. This elemental composition not only ensures its safety for agricultural use but also enhances its value as both a nutrient carrier and a supplementary fertilizers component.

Physical characteristics of S/CRFs Granules

Uncoated S/CRFs granules prepared from biochar exhibited a compact, solid morphology, black coloration, and slightly rough surface texture, with an average mass of 0.551 g (SD = 0.0026) and density of 0.781 g/cm³ (SD = 0.0026) (Fig.-2a). These physical characteristics indicate a stable granular structure suitable for handling and further modification. To enhance nutrient release control, hydrogel coating was applied to the granules. The coated S/CRFs granules displayed a smoother surface with a thin whitish layer covering the biochar matrix (Fig.-2b), consistent with successful hydrogel encapsulation. The coated granules showed a slightly higher average mass (0.654 g, SD = 0.0044) and density (0.798 g/cm³, SD = 0.0011), suggesting that the hydrogel layer contributed additional bulk while maintaining structural compactness.

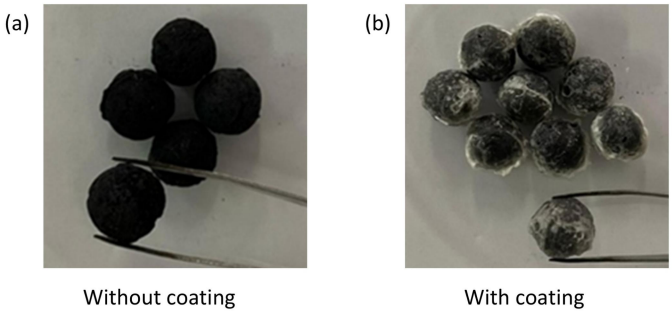


Fig.-2: Granule of S/CRFs: (a) without Coating, (b) with Coating

Three types of coated granules were prepared: (i) hydrogel-coated biochar without KCl impregnation (BC-A-G-E), (ii) hydrogel-coated biochar impregnated for 24 h (BCI_{24}-A-G-E), and (iii) hydrogel-coated biochar impregnated for 48 h (BCI_{48}-A-G-E). The successful formation of stable, compact, and coated S/CRFs granules is significant, as it ensures that the system integrates desorption properties of biochar, diffusion in the reservoir (bulk) and the diffusion-barrier function of hydrogel coating. This triple mechanism mimics the two barriers system C/RF, widely recognized as an effective strategy to extend nutrient release duration while minimizing leaching losses.[37,38] Thus, the combination of KCl-impregnated biochar with hydrogel encapsulation and coating provides a promising S/CRFs system, capable of delivering nutrients in a controlled manner through internal pore storage, reservoir, and external coating diffusion resistance.

Performance of Biochar and S/CRFs Granules

Sorption and Desorption of KCl on Biochar

The impregnation of rice husk biochar with saturated KCl solution was conducted at two contact times (24 and 48 h) to evaluate its nutrient sorption capacity**.** The results, (Table-2), show that increasing the impregnation time significantly enhanced the amount of KCl retained in the biochar, from 0.268 g (24 h) to 0.401 g (48 h). This indicates that prolonged contact allows greater diffusion of K^+ and Cl^- ions into the biochar pore network, driven by a strong concentration gradient between the saturated solution and the internal micro/mesopores. Nutrient sorption in biochar is controlled by multiple mechanisms, including ion exchange, electrostatic attraction, surface complexation, physical adsorption, and pore filling.[39,40] In the case of KCl, the process is dominated by capillary-driven pore filling and electrostatic interactions between K^+ ions and surface functional groups, supported by the relatively high surface area and pore volume of the rice husk biochar.

Table-2: Impregnation of Rice Husk-Derived Biochar (RHB) with KCl

Samples Code	Time of Impregnation (h)	Mass of BC (g)	Volume of saturated KCl (mL)	Mass of KCl inside BC (g)
BCI_{24}	24	5	50.0	0.2680
BCI_{48}	48	5	50.0	0.4014

These findings suggest that biochar can act as a nutrient reservoir, storing fertilizers salts in its porous matrix. To confirm the storage and release capacity of the impregnated biochar, desorption tests were performed in deionized water, with conductivity measured as an indirect indicator of KCl release (Fig.-3).

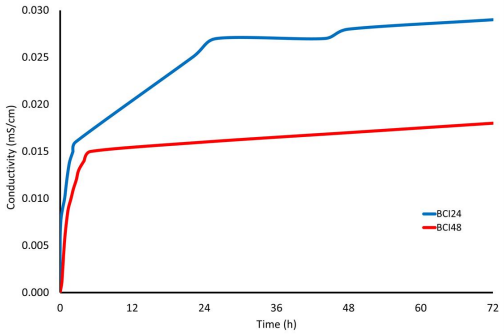


Fig.-3: Desorption of KCl from Rice Husk-Derived Biochar (RHB) into Deionized Water

Both impregnated samples released ions into the medium, as evidenced by a gradual increase in solution conductivity over time. Interestingly, BCI_{24} exhibited a higher conductivity increase compared to BCI_{48}, suggesting that a larger fraction of the absorbed ions was readily released from the 24 h impregnated biochar. By contrast, ions sorbed during 48 h impregnation penetrated deeper into the biochar pore structure, leading to stronger retention and slower release. The release mechanism can be explained as a three-step process: (i) water infiltration into biochar pores, (ii) dissolution of impregnated KCl, and (iii) diffusion of K^+ and Cl^- ions into the external medium. This desorption process reflects the controlled nutrient release function of biochar, in which nutrient availability is gradually modulated by water access and pore diffusion resistance. These results confirm that rice husk biochar can serve as an efficient sorbent–reservoir system for KCl, with tuneable release dynamics depending on impregnation conditions.

Swelling Ratio (SR) of S/CRFs Granules

The swelling ratio (*SR*) of BC-A-G-E, BCI_{24}-A-G-E, and BCI_{48}-A-G-E is 219.30%, 216.21%, and 208.31% respectively. These *SR* values followed the order BC-A-G-E > BCI_{24}-A-G-E > BCI_{48}-A-G-E, indicating that non-impregnated biochar facilitated the highest swelling capacity, while prolonged KCl impregnation (48 h) resulted in the lowest values. This trend can be attributed to the pore accessibility of the biochar within the granule matrix. In the non-impregnated state, biochar retained open mesopores and micropores that allowed maximum water infiltration and hydrogel expansion. Conversely, partial or full impregnation of biochar with KCl progressively filled the porous network, restricting water uptake and reduced osmotic driving force. Longer impregnation time promoted greater ion diffusion into biochar, reducing the void space available for hydration. Consequently, water mass uptake (W_t) decreased, lowering *SR* values. Thus, although impregnation enhances nutrient loading, excessive duration compromises the hydrogel swelling performance, highlighting the trade-off between nutrient encapsulation and water absorption.

Water Retention (WR) of S/CRFs Granules

Water retention (WR) over 120 h revealed.an exponential decline in moisture content across all treatments (Fig.-4), reflecting natural evaporation and diffusion. Non-impregnated granules showed slightly higher *WR* values compared to impregnated ones, particularly during the initial stages. This effect is attributed to the higher pore accessibility of untreated biochar, which slowed water release.

In contrast, 24 h and 48 h impregnated granules exhibited faster water depletion due to pore blockage by KCl, limiting storage capacity and accelerating desorption. When integrated with *SR*, *WR* provides a

holistic view of water dynamics in the S/CRFs system. *SR* indicates hydrogel swelling potential, and *WR* evaluates temporal stability of retained water.

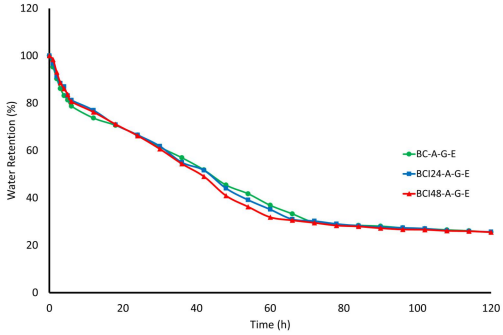


Fig.-4: Water Retention (*WR*) of Coated S/CRFs Granule

The collective decline of these parameters in impregnated granules underscores the trade-off between nutrient enrichment and hydration capacity. Optimising impregnation conditions is therefore crucial to balance nutrient loading with sufficient water storage and sustained release, ensuring efficient performance of S/CRFs formulations in agricultural applications.

Release Behaviour of KCl from S/CRFs Granule into Deionised Water

The experimental results for the release behaviour of KCl from S/CRFs granules into deionised water (Fig.-5) showed six distinct release profiles, resulting from the combination of two factors: impregnation time (non-impregnated, 24 h, and 48 h) and hydrogel coating (uncoated vs. coated).

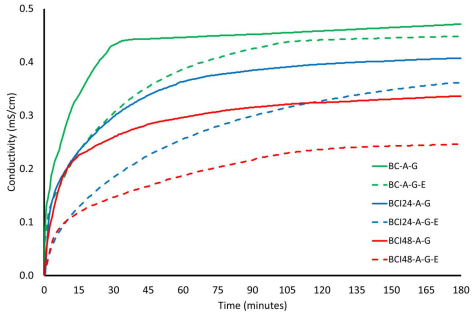


Fig.-5: Release Behaviour of KCl from S/CRFs Granule into Deionised Water

In general, all treatments exhibited an increase in conductivity with time, but the release rates varied significantly. Non-impregnated-uncoated granules (BC-A-G) released KCl most rapidly, showing a sharp conductivity increase characteristic of conventional fertilizers, which tend to release nutrients without control. The application of a poly(vinyl alcohol)/borate/alginate (PVA/B/A) hydrogel as the coater for the same granule (BC-A-G-E) slowed nutrient release markedly, demonstrating its effectiveness as a physical diffusion barrier. Granules impregnated for 24 h (BCI_{24}-A-G) exhibited slower release compared to the non-impregnated formulation (BC-A-G), as part of the KCl was embedded within the biochar micropores, requiring a longer diffusion pathway before reaching the bulk solution. When combined with hydrogel coating (BCL_{24}-A-G-E), the release rate was further reduced due to the presence of triple diffusion barriers. The most controlled release was observed in granules impregnated for 48 h with hydrogel coating (BCI_{48}-A-G-E), which showed the lowest final conductivity value. This indicates a multi-stage release mechanism, where ions are first retained within the microporous biochar matrix and subsequently retarded by the external hydrogel network both in the form of matrix (bulk) and reservoir (coater). The release mechanism of KCl from the S/CRFs into deionised water can be explained as follows. In the non-impregnated, uncoated granules (BC-A-G), KCl was present only within the bulk matrix (reservoir system). Upon water penetration, the KCl readily dissolved and diffused into the surrounding solution, resulting in a rapid increase in electrical conductivity. In contrast, the S/CRFs prepared using KCl-impregnated biochar and subsequently mixed with and coated by hydrogel (BCI_X-A-G-E) exhibited sequential diffusion barriers. Specifically, the released KCl had to diffuse through the biochar micropores,

the hydrogel matrix, and finally the polymer coating, resulting in slower and more gradual release kinetics. After the equilibrium or saturation condition is reached, non-impregnated granules (BC-A-G) reached a conductivity of 0.448 mS, while impregnated granules showed markedly lower values: 0.361 mS (BCI_{24}-A-G) and 0.246 mS (BCI_{48}-A-G). The phenomenon is similar for both the granule with and without coating (BCI_{24}-A-G-E and BCI_{48}-A-G-E). This reduction reflects a decrease in immediately soluble KCl due to entrapment within biochar pores, thereby extending nutrient availability. This study demonstrates that the combination of biochar impregnation, reservoir, and hydrogel coating creates a synergistic multi-barrier system, enhancing the temporal control of nutrient release. Biochar functions as an ion adsorbent, whereas the hydrogel serves both as a nutrient reservoir and as an external diffusion-controlling barrier. Together, these components establish a hierarchical release mechanism that delays ion transport and minimises nutrient losses. This integrated design represents a step toward the development of smart fertilizers capable of synchronising nutrient release with plant demand while reducing nutrient losses to the environment, particularly under conditions susceptible to leaching.

Release Behaviour of KCl from S/CRFs Granule into Soil

The release profile of KCl from S/CRFs granules into soil is shown in Fig.-6. The release curve demonstrates a biphasic pattern, consisting of an initial burst followed by a sustained release phase. At the initial stage (0–12 h), approximately 25.03% of potassium was released, exceeding the recommended maximum of 15% within 24 h for slow/controlled-release fertilizers (S/CRFs).[41] By day 1, cumulative release reached 42.91%, and increased steadily to 75.59% by day 7. Subsequently, the release rate declined, reaching 81% at day 14, 83.76% at day 28, and 89.47% at day 42.

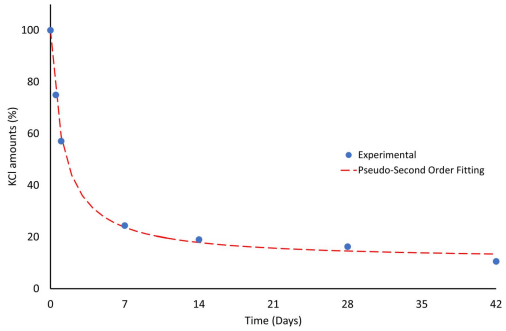


Fig.-6: Release Behaviour of KCl from S/CRFs Granule into Soil

Comparative analysis with previous studies supports these findings. It was reported that single impregnation techniques led to phosphorus release of up to 40% within 5 days.[42] It was also observed that extremely rapid release occurred from single-granule fertilizers (53.62% K and 49.62% P within 24 h).[43] By contrast, the integration of biochar impregnation, granulation, and hydrogel coating in this study produced a more moderate release profile, particularly after the first week. In order to determine the release mechanism of KCl onto the soil, the data were fitted to several kinetic models. To simplify the modelling and reduce the number of parameters to estimate, the data was then normalised as a percentage with regard to the initial amount of KCl in the hydrogel, which is 231.74 g mL^{-1}. Statistical analysis of the release of KCl onto soil showed that the experimental data best fit the pseudo-second order (PSO) kinetic model with a coefficient of determination (R^2) of 0.9973, expressed in eqn.-3.

$$q_t = q_e + \frac{(1 - q_e)}{(1 - q_e)\,kt + 1} \tag{3}$$

Where q_t is the amount of KCl remaining in the granule at time t, q_e is the amount of KCl remaining in the granule after the equilibrium is reached, and k is the rate constant. PSO release kinetics typically indicate a complex mechanism of release from the hydrogel, with a limit as to how much of the available nutrient can be released from the hydrogel. The PSO kinetic model estimates that the equilibrium amount of nutrient is 10.99%, which is in line with the experimental data at day 42 of 10.53%, indicating that after 6 weeks all the releasable nutrients had been released from the hydrogel to soil.

Biodegradability

In this study, granules were exposed to activated sludge as a microbial source, and surface changes were visually monitored over 70 days (Fig.-7).

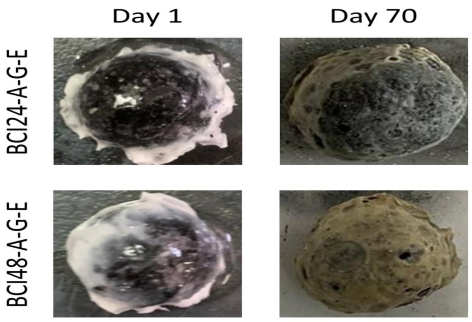


Fig.-7: Photograph of Physical Appearance of BCI_{48}-A-G-E and BCI_{24}-A-G-E During Biodegradability Test

At day 1, both 24 h and 48 h impregnated granules appeared intact, with smooth surfaces and no visible degradation. By day 30, initial signs of surface deterioration were observed. Granules impregnated for 24 h exhibited subtle discolouration, while 48 h impregnated samples showed more pronounced changes, including roughened surfaces, increased porosity, and yellow–brown discolouration. By day 70, advanced degradation was evident in both formulations, characterised by hydrogel softening and microbial biofilm growth. These results demonstrate that structural degradation begins approximately in the fourth week, coinciding with the transition from diffusion-dominated release to matrix-assisted release, thereby aligning degradation dynamics with nutrient supply. This synchronisation is beneficial, as it ensures that nutrient release accelerates during later plant growth stages, when nutrient demand is typically higher.[41,44] The observed biodegradability is attributed to the material composition of the granules. Hydrogels composed of PVA, borate, and alginate are known to be microbially degradable.[44] In addition, rice husk biochar provides a porous substrate that supports microbial colonisation.[45] Furthermore, longer impregnation times (48 h) appeared to increase porosity and accessibility of the matrix to microbial attack, explaining the more rapid structural deterioration observed in these samples. The degradation pathway involves a combination of hydrolytic and microbial processes, with biochar serving not only as a nutrient reservoir but also as a microhabitat for microbial consortia. This dual functionality ensures that the S/CRFs granules not only release nutrients in a controlled manner but also decompose naturally, leaving no harmful residues. Such biodegradability is essential for the design of sustainable, environmentally friendly fertilizers, aligning with circular economy principles and soil health preservation.[46] It also supports the objectives of the United Nations Sustainable Development Goals (SDGs), particularly SDG 12 (Responsible Consumption and Production).

CONCLUSION

Although the incorporation of rice husk-derived biochar (RHB) into the PVA/borate/alginate hydrogel matrix did not significantly affect the swelling ratio or water retention capacity, it effectively integrated nutrient storage, controlled release, and biodegradability into a single material system. Impregnation of RHB with KCl significantly enhanced its nutrient storage capacity, and a longer impregnation time (48 h) resulted in greater K^+ retention and a slower release rate than the 24 h treatment. Using the hydrogel as both a binder and a coating produced compact, mechanically stable granules with properties suitable for agricultural application. In aqueous media, hydrogel-coated granules prepared with KCl-impregnated biochar exhibited substantially slower nutrient release than the uncoated controls. In soil, nutrient release reached 25.03% during the first 12 hours and gradually increased to 89.47% after 42 days. Among the kinetic models evaluated, the pseudo-second-order model provided the best fit to the experimental data. The granules also exhibited progressive microbial and hydrolytic degradation, beginning around day 30 and progressing to substantial softening by day 70. The integration of KCl-impregnated biochar, a hydrogel reservoir, and a hydrogel coating provided a promising smart fertilizer platform that combines controlled nutrient release with environmentally benign biodegradation. This system shows strong

potential for precision agriculture, particularly in regions susceptible to nutrient leaching or irregular rainfall, and thereby supports the achievement of the objectives of Sustainable Development Goal 12 (Responsible Consumption and Production).

ACKNOWLEDGMENTS

We are grateful to Universitas Pendidikan Indonesia for the funding of this research via the "Penelitian Pengembangan Kelompok Bidang Keilmuan" scheme (Contract number: 220/UN40.D/PT.01.01/2025).

CONFLICT OF INTERESTS

The authors declare that there is no conflict of interest.

AUTHOR CONTRIBUTIONS

The present work is related to *SDG-12: Responsible Consumption and Production*. All the authors contributed significantly to this manuscript, participated in reviewing/editing and approved the final draft for publication. The research profile of the authors can be verified from their ORCID ids, given below:

H. Hendrawan https://orcid.org/0000-0003-2439-6671
A.R. Idauli https://orcid.org/0009-0008-4135-7758
H.A. Aziz https://orcid.org/0000-0002-6825-4539
F. Khoerunnisa https://orcid.org/0000-0002-0198-756X

Open Access: This article is distributed under the terms of the Creative Commons Attribution 4.0 International License (http://creativecommons.org/licenses/by/4.0/), which permits unrestricted use, distribution, and reproduction in any medium, provided you give appropriate credit to the original author(s) and the source, provide a link to the Creative Commons license, and indicate if changes were made.
Cite this article as: Hendrawan *et al.*, *Rasayan J. Chem.*, 19(4), 2276-2287(2026), https://doi.org/10.31788/RJC.2026.1949880

REFERENCES

1. H. Mansouri, H.A. Said, H. Noukrati, A. Oukarroum, H.B. Youcef and F. Perreault, *Advanced Sustainable Systems*, **7,** 2300149(2023), https://doi.org/10.1002/adsu.202300149
2. S. Govil, N.V.D. Long, M. Escribà-Gelonch and V. Hessel, *Industrial Crops and Products*, **219**, 119160(2024), https://doi.org/10.1016/j.indcrop.2024.119160
3. L. Chen, Q. Chen, P. Rao, L. Yan, A. Shakib and G. Shen, *Sustainability,* **10**, 2740(2018), https://doi.org/10.3390/su10082740
4. T. Tan, Y. Xu, X. Liao, Z. Ti and S. Xue, *Global Change Biology Bioenergy*, **16**, e13142(2024), https://doi.org/10.1111/gcbb.13142
5. A. Gamage, B. Basnayake, J.D. Costa and O. Merah, *Plants,* **11**, 75(2021), https://doi.org/10.3390/plants11010075
6. Y. Song, L. Ma, Q. Duan, H. Xie, X. Dong, H. Zhang and L. Yu, *Molecules*, **29**, 4835(2024), https://doi.org/10.3390/molecules29204835
7. A.F. Chamorro, M. Palencia and E.M. Combatt, *Polymers,* **17**, 1117(2025), https://doi.org/10.3390/polym17081117
8. X. Liang, H.J. Zhong, H. Ding, B. Yu, X. Ma, X. Liu, C.M. Chong and J. He, *Polymers*, **16**, 2755(2024), https://doi.org/10.3390/polym16192755
9. N. Wang, B. Wang, Y. Wan, B. Gao and V.D. Rajput, *Journal of Environmental Management*, **348,** 119133(2023), https://doi.org/10.1016/j.jenvman.2023.119133
10. R. Betriani, S. Sutarno, I. Kartini and J. Budiarta, *Indonesian Journal of Chemistry*, **23**, 184-199(2023), https://doi.org/10.22146/ijc.76205
11. I. Dere, D.T. Gungula, S.A. Kareem, F.P. Andrew, A.M. Saddiq, V.T. Tame, H.M. Kefas, D.O. Patrick and J.I. Joseph, *Heliyon*, **11**, e42036(2025), https://doi.org/10.1016/j.heliyon.2025.e42036
12. M.R. Khatun, M.A.K. Azad and M.I.H. Mondal, *International Journal of Biological Macromolecules*, **313,** 144295(2025), https://doi.org/10.1016/j.ijbiomac.2025.144295
13. L.R. Yuan, L. Ren, X. Tian, Z. Huang, Y. Xiao, S. Wei and Z. Wang, *RSC Advances,* **6**, 71425(2016), https://doi.org/10.1039/C6RA14032G

14. W. Po-Hsun, C. Yin-Ru and L. Duu-Jong, *Journal of the Taiwan Institute of Chemical Engineers*, **103**, 85(2019), https://doi.org/10.1016/j.jtice.2019.07.013
15. H.T.B.M. Petrus, A.D.P. Putera, I.P. Wangi, M.A. Ramadhian, H. Setiawan and A. Prasetya, *International Journal of Technology*, **11**, 774(2020), https://doi.org/10.14716/ijtech.v11i4.3520
16. C.E. Brewer, K. Schmidt-Rohr, J.A. Satrio and R.C. Brown, *Environmental Progress & Sustainable Energy,* **28**, 386(2009), https://doi.org/10.1002/ep.10378
17. M. Keiluweit, P.S. Nico, M. Johnson and M. Kleber, *Environmental Science & Technology,* **44**, 1247(2010), https://doi.org/10.1021/es9031419
18. D. Chen, J. Zhou and Q. Zhang, *Bioresource Technology*, **169**, 313(2014), https://doi.org/10.1016/j.biortech.2014.07.009
19. M. Ahmad, A.U. Rajapaksha, J.E. Lim, M. Zhang, N. Bolan, D. Mohan, M. Vithanage, S.S. Lee and Y.S. Ok, *Chemosphere,* **99**, 19(2014), https://doi.org/10.1016/j.chemosphere.2013.10.071
20. J. Guo and B. Chen, *Environmental Science & Technology,* **48**, 9103(2014), https://doi.org/10.1021/es405647e
21. A. Mukherjee, A.R. Zimmerman and W. Harris, *Geoderma,* **163**, 247(2011), https://doi.org/10.1016/j.geoderma.2011.04.021
22. L. Han, L. Qian, J. Yan and M. Chen, *Environmental Science and Pollution Research*, **24**, 5554(2017), https://doi.org/10.1007/s11356-016-8303-8
23. S.K. Sharma, G. Sharma, A. Sharma, K. Bhardwaj, K. Preeti, K. Singh, A. Kumar, V.K. Pal, E.H. Choi, S.P. Singh and N.K. Kaushik, *Applied Surface Science Advances*, **8**, 100225(2022), https://doi.org/10.1016/j.apsadv.2022.100225
24. M.Z. Suhot, M.Z. Hassan, S.A. Aziz and M.Y.M. Daud, *Polymers*, **13**, 2391(2021), https://doi.org/10.3390/polym13152391
25. M.A. Azmi, N.A.A. Ismail, M. Rizamarhaiza, W.M. Hasif and H. Taib, *AIP Confererence Proceedings*, **1756**, 020005(2016), https://doi.org/10.1063/1.4958748
26. T. H. Liou, *Materials Science and Engineering: A,* **364**, 313(2004), https://doi.org/10.1016/j.msea.2003.08.045
27. A. Tadjarodi, M. Haghverdi and V. Mohammadi, *Materials Research Bulletin*, **47**, 2584(2012), https://doi.org/10.1016/j.materresbull.2012.04.143
28. J.H. Yuan, R.K. Xu and H. Zhang, *Bioresource Technology,* **102**, 3488(2011), https://doi.org/10.1016/j.biortech.2010.11.018
29. Y. Chen, X. Zhang, W. Chen, H. Yang and H. Chen, *Bioresource Technology*, **246**, 101(2017), https://doi.org/10.1016/j.biortech.2017.08.138
30. D. Dong, C. Wang, L. Van Zwieten, H. Wang, P. Jiang, M. Zhou and W. Wu, *Journal of Soils and Sediments*, **20**, 3027(2020), https://doi.org/10.1007/s11368-019-02401-8
31. Y. Jia, S. Shi, J. Liu, S. Su, Q. Liang, X. Zeng and T. Li, *Applied Sciences*, **8**, 1019(2018), https://doi.org/10.3390/app8071019
32. X. Liu, J. Liao, H. Song, Y. Yang, C. Guan and Z. Zhang, *Scientific Reports*, **9**, 9548(2019), https://doi.org/10.1038/s41598-019-46065-3
33. S. Mopoung, V. Udeye, S. Viruhpintu, N. Yimtragool and V. Unhong, *The Scientific World Journal*, **2020**, 7901362(2020), https://doi.org/10.1155/2020/7901362
34. D.N.V. Gamage, R.B. Mapa, R.S. Dharmakeerthi and A. Biswas, *Soil Research*, **54**, 302(2016), https://doi.org/10.1071/SR15102
35. S. Alejandro, S. Höller, B. Meier and E. Peiter, *Frontiers in Plant Science*, **11**, 1(2020), https://doi.org/10.3389/fpls.2020.00300
36. S. Kumar, S. Kumar and T. Mohapatra, *Frontiers in Plant Science*, **12**, 1(2021). https://doi.org/10.3389/fpls.2021.665583
37. W. Shi, Y. Ju, R. Bian, L. Li, S. Joseph, D.R.G. Mitchell, P. Munroe, S. Taherymoosavi and G. Pan, *Science of the Total Environment*, **701**, 134424(2020), https://doi.org/10.1016/j.scitotenv.2019.134424
38. W. Luo, L. Qian, W. Liu, X. Zhang, Q. Wang, H. Jiang, B. Cheng, H. Ma and Z. Wu, *Science of the Total Environment*, **768**, 144454(2021), https://doi.org/10.1016/j.scitotenv.2020.144454

39. X. Tan, Y. Liu, G. Zeng, X. Wang, X. Hu, Y. Gu and Z. Yang, *Chemosphere*, **125**, 70(2015), https://doi.org/10.1016/j.chemosphere.2014.12.058
40. D. Mohan, A. Sarswat, Y.S. Ok and C.U. Pittman Jr, *Bioresource Technology*, **160**, 191(2014), https://doi.org/10.1016/j.biortech.2014.01.120
41. M.E. Trenkel, *Slow- and Controlled-Release and Stabilized Fertilizers: An Option for Enhancing Nutrient Use Efficiency in Agriculture*, International Fertilizer Industry Association (IFA) Paris, France, p.15 (2010).
42. C. Sepúlveda-Cadavid, J.H. Romero, M. Torres, E. Becerra-Agudelo and J.E. López, *Journal of Soil Science and Plant Nutrition*, **21**, 2980(2021), https://doi.org/10.1007/s42729-021-00583-0
43. P. Kim, D. Hensley and N. Labbé, *Geoderma*, **232–234**, 341(2014), http://doi.org/10.1016/j.geoderma.2014.05.017
44. Q. Chen, Q. Ding, W. Li, J. Deng, Q. Lin and J. Li, *Bioresource Technology*, **347**, 126741(2022), https://doi.org/10.1016/j.biortech.2022.126741
45. S. Khajavi-Shojaei, A. Moezzi, M.N. Masir and M. Taghavi, *Biomass Conversion and Biorefinery*, **13**, 593(2023), https://doi.org/10.1007/s13399-020-01137-7
46. G.V. Subbarao, K.L. Sahrawat, K. Nakahara, T. Ishikawa, M. Kishii, I.M. Rao, C.T. Hash, T.S. George, P.S. Rao, P. Nardi, D. Bonnett, W. Berry, K. Suenaga and L.C. Lata, *Advances in Agronomy*, **160**, 249(2020), https://doi.org/10.1016/B978-0-12-394275-3.00001-8

[RJC-9880/2026]